

# Northumbria Research Link

Citation: Stubbins, Aron, Spencer, Robert, Mann, Paul, Holmes, Robert, McClelland, James, Niggemann, Jutta and Dittmar, Thorsten (2015) Utilizing Colored Dissolved Organic Matter to Derive Dissolved Black Carbon Export by Arctic Rivers. *Frontiers in Earth Science*, 3 (63). ISSN 2296-6463

Published by: Nature

URL: <http://journal.frontiersin.org/article/10.3389/feart.2015.00063/abstract>

This version was downloaded from Northumbria Research Link:  
<http://nrl.northumbria.ac.uk/23930/>

Northumbria University has developed Northumbria Research Link (NRL) to enable users to access the University's research output. Copyright © and moral rights for items on NRL are retained by the individual author(s) and/or other copyright owners. Single copies of full items can be reproduced, displayed or performed, and given to third parties in any format or medium for personal research or study, educational, or not-for-profit purposes without prior permission or charge, provided the authors, title and full bibliographic details are given, as well as a hyperlink and/or URL to the original metadata page. The content must not be changed in any way. Full items must not be sold commercially in any format or medium without formal permission of the copyright holder. The full policy is available online: <http://nrl.northumbria.ac.uk/policies.html>

This document may differ from the final, published version of the research and has been made available online in accordance with publisher policies. To read and/or cite from the published version of the research, please visit the publisher's website (a subscription may be required.)

[www.northumbria.ac.uk/nrl](http://www.northumbria.ac.uk/nrl)



# Utilizing Colored Dissolved Organic Matter to Derive Dissolved Black Carbon Export by Arctic Rivers

Aron Stubbins<sup>1\*</sup>, Robert Spencer<sup>2</sup>, Paul J. Mann<sup>3</sup>, R. M. Holmes<sup>4</sup>, James McClelland<sup>5</sup>, Jutta Niggemann<sup>6</sup>, Thorsten Dittmar<sup>6</sup>

<sup>1</sup>Skidaway Institute of Oceanography, University of Georgia, USA, <sup>2</sup>Florida State University, USA, <sup>3</sup>Northumbria University, United Kingdom, <sup>4</sup>Woods Hole Research Center, USA, <sup>5</sup>University of Texas Marine Science Institute, USA, <sup>6</sup>University of Oldenburg, Germany

**Submitted to Journal:**  
Frontiers in Earth Science

**Specialty Section:**  
Marine Biogeochemistry

**Article type:**  
Original Research Article

**Manuscript ID:**  
167592

**Received on:**  
02 Sep 2015

**Revised on:**  
29 Sep 2015

**Frontiers website link:**  
[www.frontiersin.org](http://www.frontiersin.org)

### ***Conflict of interest statement***

**The authors declare that the research was conducted in the absence of any commercial or financial relationships that could be construed as a potential conflict of interest**

### ***Author contribution statement***

All authors contributed to the design of the study. JN analyzed samples for dissolved black carbon. AS, RGMS, and PJM conducted modeling studies. All authors contributed to the writing of the manuscript.

### ***Keywords***

Carbon Cycle, Arctic, black carbon, Colored dissolved organic matter (CDOM), Climate Change, Rivers, hydrology

### ***Abstract***

Word count: 324

Wildfires have produced black carbon (BC) since land plants emerged. Condensed aromatic compounds, a form of BC, have accumulated to become a major component of the soil carbon pool. Condensed aromatics leach from soils into rivers, where they are termed dissolved black carbon (DBC). The transport of DBC by rivers to the sea is a major term in the global carbon and BC cycles. To estimate Arctic river DBC export, 25 samples collected from the six largest Arctic rivers (Kolyma, Lena, Mackenzie, Ob', Yenisey and Yukon) were analyzed for dissolved organic carbon (DOC), colored dissolved organic matter (CDOM), and DBC. A simple, linear regression between DOC and DBC indicated that DBC accounted for  $8.9 \pm 0.3\%$  DOC exported by Arctic rivers. To improve upon this estimate, an optical proxy for DBC was developed based upon the linear correlation between DBC concentrations and CDOM light absorption coefficients at 254 nm ( $a_{254}$ ). Relatively easy to measure  $a_{254}$  values were determined for 410 Arctic river samples between 2004 and 2010. Each of these  $a_{254}$  values was converted to a DBC concentration based upon the linear correlation, providing an extended record of DBC concentration. The extended DBC record was coupled with daily discharge data from the six rivers to estimate riverine DBC loads using the LOADEST modeling program. The six rivers studied cover 53% of the pan-Arctic watershed and exported  $1.5 \pm 0.1$  million tons of DBC per year. Scaling up to the full area of the pan-Arctic watershed, we estimate that Arctic rivers carry  $2.8 \pm 0.3$  million tons of DBC from land to the Arctic Ocean each year. This equates to ~8% of Arctic river DOC export, slightly less than indicated by the simpler DBC vs DOC correlation-based estimate. Riverine discharge is predicted to increase in a warmer Arctic. DBC export was positively correlated with river runoff, suggesting that the export of soil BC to the Arctic Ocean is likely to increase as the Arctic warms.

### ***Ethics statement***

(Authors are required to state the ethical considerations of their study in the manuscript including for cases where the study was exempt from ethical approval procedures.)

*Did the study presented in the manuscript involve human or animal subjects:* No

# Utilizing Colored Dissolved Organic Matter to Derive Dissolved Black Carbon Export by Arctic Rivers

Aron Stubbins<sup>1\*</sup>, Robert G. M. Spencer<sup>2</sup>, Paul J. Mann<sup>3</sup>, R. Max Holmes<sup>4</sup>, James W. McClelland<sup>5</sup>, Jutta Niggemann<sup>6</sup>, Thorsten Dittmar<sup>6</sup>

<sup>1</sup>Skidaway Institute of Oceanography, Department of Marine Sciences, University of Georgia, Savannah, GA 31411, USA

<sup>2</sup>Department of Earth, Ocean and Atmospheric Science, Florida State University, Tallahassee, FL 32306, USA

<sup>3</sup>Department of Geography, Northumbria University, Newcastle-upon-Tyne, UK

<sup>4</sup>Woods Hole Research Center, 149 Woods Hole Road, Falmouth, MA 00540, USA

<sup>5</sup>University of Texas Marine Science Institute, 750 Channel View Drive, Port Aransas, TX 78373, USA

<sup>6</sup>Research Group for Marine Geochemistry, University of Oldenburg, Institute for Chemistry and Biology of the Marine Environment, Carl-von-Ossietzky-Str. 9-11, 26129 Oldenburg, Germany

**\*Correspondence:** Dr. Aron Stubbins. Skidaway Institute of Oceanography, Department of Marine Sciences, University of Georgia, 10 Ocean Science Circle, Savannah, GA 31411, USA. aron.stubbins@skio.uga.edu

**Keywords:** Carbon Cycle, Arctic, Black Carbon, Colored Dissolved Organic Matter (CDOM), Climate Change, Rivers, Hydrology.

## Abstract

Wildfires have produced black carbon (BC) since land plants emerged. Condensed aromatic compounds, a form of BC, have accumulated to become a major component of the soil carbon pool. Condensed aromatics leach from soils into rivers, where they are termed dissolved black carbon (DBC). The transport of DBC by rivers to the sea is a major term in the global carbon and BC cycles. To estimate Arctic river DBC export, 25 samples collected from the six largest Arctic rivers (Kolyma, Lena, Mackenzie, Ob', Yenisey and Yukon) were analyzed for dissolved organic carbon (DOC), colored dissolved organic matter (CDOM), and DBC. A simple, linear regression between DOC and DBC indicated that DBC accounted for  $8.9 \pm 0.3\%$  DOC exported by Arctic rivers. To improve upon this estimate, an optical proxy for DBC was developed based upon the linear correlation between DBC concentrations and CDOM light absorption coefficients at 254 nm ( $a_{254}$ ). Relatively easy to measure  $a_{254}$  values were determined for 410 Arctic river samples between 2004 and 2010. Each of these  $a_{254}$  values was converted to a DBC concentration based upon the linear correlation, providing an extended record of DBC concentration. The extended DBC record was coupled with daily discharge data from the six rivers to estimate riverine DBC loads using the LOADEST modeling program. The six rivers studied cover 53% of the pan-Arctic watershed and exported  $1.5 \pm 0.1$  million tons of DBC per year. Scaling up to the full area of the pan-Arctic watershed, we estimate that Arctic rivers carry  $2.8 \pm 0.3$  million tons of DBC from land to the Arctic Ocean each year. This equates to  $\sim 8\%$  of Arctic river DOC export, slightly less than indicated by the simpler DBC vs DOC correlation-based estimate. Riverine discharge is predicted to increase in a warmer Arctic. DBC export was positively correlated with

42 river runoff, suggesting that the export of soil BC to the Arctic Ocean is likely to increase as the  
43 Arctic warms.

## 44 **1.Introduction**

45 Fire occurs in nearly all terrestrial ecosystems (Bowman et al., 2009) and is on the increase in the  
46 Arctic (Higuera et al., 2008;Hu et al., 2010). Black carbon (BC) refers to thermally altered  
47 organic material and it comes in many forms (Forbes et al., 2006), ranging in chemistry from  
48 minimally charred biomolecules (Myers - Pigg et al., 2015) to condensed aromatics formed at  
49 high temperatures (Dittmar, 2008). Once formed, condensed aromatics are ultra-refractory within  
50 soils, being preferentially preserved for hundreds to thousands of years (Schmidt et al., 2011).  
51 This stability, together with the ubiquity of fire, has resulted in condensed aromatics being  
52 distributed throughout the world's soils (Forbes et al., 2006;Guggenberger et al., 2008), where  
53 they have accumulated to represent approximately 10% of the global soil carbon store (Mitra et  
54 al., 2013). Wildfires have burned since the emergence of land plants 420 million years ago  
55 (Bowman et al., 2009). Without a significant loss term, condensed aromatics should have  
56 accumulated to represent an even greater pool of soil carbon than currently observed. The  
57 mobilization of soil condensed aromatics into solution and subsequent export by rivers to the  
58 oceans is the main loss term identified to date (Guggenberger et al., 2008;Dittmar et al.,  
59 2012a;Jaffé et al., 2013).

60 Once in solution, condensed aromatics are termed dissolved black carbon (DBC) (Dittmar,  
61 2008) and their export through rivers links the soil BC store to another major global carbon store,  
62 that of dissolved organic carbon (DOC) in the oceans (Hansell, 2013). As in soils, DBC in the  
63 oceans appears to be highly bio-refractory, based upon its ancient apparent radiocarbon age  
64 (Ziolkowski and Druffel, 2010), and has accumulated to be major pool of global carbon (>12,000  
65 Tg-C; Tg-C =  $10^{12}$  grams of carbon) (Dittmar and Paeng, 2009). Deep sea hydrothermal systems  
66 (Dittmar and Paeng, 2009) and atmospheric deposition (Jurado et al., 2008) have been proposed  
67 as sources of oceanic DBC. However, rivers are currently the major identified source of DBC to  
68 the ocean, delivering an estimated 26.5 Tg of DBC per year (Jaffé et al., 2013). Photo-  
69 degradation by sunlight is the major identified sink for DBC (Stubbins et al., 2010;Stubbins et  
70 al., 2012). However, at depth in the ocean, DBC behaves almost conservatively, suggesting  
71 minimal loss when light is not present (Dittmar and Paeng, 2009). Therefore, if DBC can reach  
72 areas of deep water formation before being photo-degraded, it may be in essence reburied in the  
73 deep ocean.

74 In this manuscript we present data for DBC concentrations in major Arctic rivers and  
75 estimate annual export of DBC from Arctic soils to the Arctic Ocean. While riverine inputs of  
76 DOC to the Arctic Ocean are well constrained (Raymond et al., 2007;Spencer et al.,  
77 2009;Holmes et al., 2012), this is the first estimate of DBC export to the Arctic Ocean. To make  
78 this estimate, we quantified DBC in depth and flow integrated samples collected near the mouths  
79 of the six largest Arctic rivers under variable hydrological conditions (Figure 1; Kolyma, Lena,  
80 Mackenzie, Ob', Yenisey and Yukon). Together, these six river watersheds cover 53% of the  
81 pan-Arctic watershed (Holmes et al., 2012). Discharge varies markedly with season in Arctic  
82 rivers. In winter, November to April, the watersheds and river surfaces are frozen such that  
83 groundwater derived discharge dominates, and only 10 to 15% of the annual Arctic river DOC  
84 load is exported during this six month period (Holmes et al., 2012). With the warmth of spring,  
85 thawing winter snow and ice drive a massive discharge peak that is accompanied by highest  
86 annual DOC concentrations. As a consequence, typically 45 to 65% of the annual Arctic DOC

87 load is exported during May and June, the two months of the spring freshet (Raymond et al.,  
88 2007;Spencer et al., 2009;Holmes et al., 2012). After the intense spring freshet, the months from  
89 July through October account for the remainder of the annual DOC export.

90 In the current study, DBC was quantified in 25 samples, collected over a broad range of  
91 runoff values in 2009. We also determined the Napierian light absorption coefficient of colored  
92 DOM ( $a_{CDOM}$ ;  $m^{-1}$ ), an optical property of DOM that is a good proxy for the aromatic  
93 components of the DOM pool (Weishaar et al., 2003;Stubbins et al., 2008;Spencer et al., 2009),  
94 including DBC (Stubbins et al., 2012).  $a_{CDOM}$  was determined for 410 samples spanning the  
95 seasonal hydrographs of each river and seven years (2004 to 2010). The utility of  $a_{CDOM}$  as a  
96 proxy for DBC within Arctic rivers was confirmed and used within a LOADEST modelling  
97 exercise to develop a robust estimate for DBC export to the Arctic Ocean.

## 98 **2.Methods**

### 99 **2.1 Sample collection and processing**

100 Sample sites for each river were as follows, Salekhard (Ob'), Dudinka (Yenisey), Zhigansk  
101 (Lena), Cherskiy (Kolyma), Pilot Station (Yukon) and Tsiigehtchic (Mackenzie). Discharge data  
102 ( $m^3 sec^{-1}$ ) was taken from the ArcticRIMS website (<http://rims.unh.edu/data.shtml>) for nearby  
103 gauging stations and converted to surface area normalized runoff ( $m^3 km^{-2} sec^{-1}$ ; Table S1). The  
104 gauging stations and sampling locations are near the mouths of the rivers, capturing 96% of the  
105 six rivers combined watershed area (Figure 1; Table 1). Depth integrated, flow weighted samples  
106 were collected following US Geological Survey protocols, filtered through pre-cleaned capsules  
107 ( $0.45 \mu m$ ; Geotech), placed in acid-soaked Nalgene polycarbonate bottles and frozen until  
108 further processing (Holmes et al., 2012).

### 109 **2.2 Dissolved organic carbon concentrations**

110 Aliquots of sample were transferred to pre-combusted 40 mL glass vials, acidified to pH 2  
111 (hydrochloric acid), and analyzed for non-purgable organic carbon using a Shimadzu TOC-  
112 VCPH analyzer fitted with a Shimadzu ASI-V autosampler. In addition to potassium hydrogen  
113 phthalate standards, aliquots of deep seawater reference material, Batch 10, Lot# 05-10, from the  
114 Consensus Reference Material Project (CRM) were analyzed to check the precision and accuracy  
115 of the DOC analyses. Analyses of the CRM deviated by <5% from the reported value for these  
116 standards (41 to 44  $\mu M$ -DOC; <http://yyy.rsmas.miami.edu/groups/biogeochem/Table1.htm>).  
117 Routine minimum detection limits in the investigator's laboratory using the above configuration  
118 are  $2.8 \pm 0.3 \mu M$ -C and standard errors are typically  $1.7 \pm 0.5\%$  of the DOC concentration  
119 (Stubbins and Dittmar, 2012).

### 120 **2.3 Colored dissolved organic matter Napierian light absorption**

121 Sample was placed in a 1 cm quartz absorbance cell situated in the light path of an Agilent  
122 8453 ultraviolet-visible spectrophotometer and sample CDOM absorbance spectra were recorded  
123 from 190 to 800 nm. Ultrapure water (Milli-Q) provided a blank. Blank corrected absorbance  
124 spectra were corrected for offsets due to scattering and instrument drift by subtraction of the  
125 average absorbance between 700 and 800 nm (Stubbins et al., 2011). Data output from the  
126 spectrophotometer were in the form of dimensionless absorbance (i.e. optical density, OD) and  
127 were subsequently converted to the Napierian absorption coefficient,  $a$  ( $m^{-1}$ ) (Hu et al., 2002).

### 128 **2.4 Dissolved black carbon concentration and quality**

129 Freeze dried river water samples were analyzed for DBC. DBC was determined at the  
130 molecular level via the benzenepolycarboxylic acid (BPCA) method as described in (Dittmar,  
131 2008) and with modifications following (Stubbins et al., 2012). In brief, ~2  $\mu\text{mol}$  of freeze dried  
132 DOC was transferred into pre-combusted (400°C, 4 hours) 1 mL glass ampoules, and then  
133 redissolved in 500  $\mu\text{L}$  of nitric acid (65%). The ampoules were sealed and heated to 170°C in a  
134 stainless steel pressure bomb inside a furnace for 9 hours. After the ampoules cooled, 450  $\mu\text{L}$   
135 was transferred into 1 mL maximum recovery vials (Waters). The nitric acid was evaporated in a  
136 centrifugal evaporator (RVC 2-18, Christ, Germany) and the samples were redissolved in 100  $\mu\text{L}$   
137 of phosphate buffer solution ( $\text{Na}_2\text{HPO}_4$  and  $\text{NaH}_2\text{PO}_4$  each 5 mM in ultrapure water, buffered pH  
138 7.2). BPCAs were determined on a Waters ACQUITY UPLC (Ultra Performance Liquid  
139 Chromatography) system composed of a binary solvent manager, a sample manager, a column  
140 manager and a photodiode array light absorbance detector (PDA  $\epsilon\lambda$ ). BPCAs were separated on a  
141 Waters ACQUITY UPLC BEH C18 Column (2.1 x 150 mm, 1.7  $\mu\text{m}$ ) with an aqueous phase /  
142 methanol gradient. The aqueous phase consisted of a tetrabutylammonium bromide solution (4  
143 mM, ACS quality) in phosphate buffer ( $\text{Na}_2\text{HPO}_4$  and  $\text{NaH}_2\text{PO}_4$  each 5 mM in ultrapure water,  
144 pH 7.2). The injection volume was 10  $\mu\text{L}$ . BPCAs were identified according to retention time  
145 and absorbance spectra (220 to 380 nm). Quantification was performed using the absorption  
146 signal at 240 nm and external calibration.

147 DBC concentrations were calculated from the detected BPCA concentrations. The original  
148 equation to estimate DBC in nM of carbon (nM-C), from the molar BPCA concentrations of each  
149 BPCA (nM) (Dittmar, 2008) was:

$$150 \quad [\text{DBC}] = 33.4([\text{B6CA}] + [\text{B5CA}] + 0.5[\text{B4CA}] + 0.5[\text{B3CA}]) \quad (1)$$

151 The factor of 33.4 is based upon a conservative estimate of the average number of C atoms  
152 within DBC molecules identified by FT-ICR MS in a variety of natural waters (Dittmar, 2008).  
153 Note that the [DBC] is in nM-C and the BPCA concentrations are reported in nM of each  
154 molecule. Each BPCA is constituted of several C atoms. For instance, B6CA includes the 6 Cs in  
155 the aromatic ring, plus 6 carboxyl group (COOH) Cs. Therefore, the conversion factor of 33.4  
156 represents a factor of approximately 3 on a carbon basis. This compares with factors of 2.27 in  
157 an early study that assessed the yield of BPCAs from solid charcoals (Glaser et al., 1998) and a  
158 factor of 4 suggested for aquatic samples (Ziolkowski and Druffel, 2010; Ziolkowski et al.,  
159 2011). Under certain oxidation conditions the nitric acid oxidation of BC to BPCAs can yield  
160 nitrated analogs of the BPCAs that are not quantified here, but do constitute part of the DBC  
161 pool (Ziolkowski et al., 2011). Thus, the total DBC concentrations reported here represent a  
162 conservative estimate of total DBC in aquatic systems given that the conversion factor was lower  
163 than used elsewhere and nitrated-BPCAs were not included in the analysis.

164 The method used here as originally presented utilized each of the BPCAs to calculate  
165 [DBC] via equation 1 (Dittmar, 2008). Although B3CAs were reported to be stable at 170°C  
166 (Dittmar, 2008), subsequent experience suggests that recoveries of B3CAs are not always 100%  
167 (Stubbins et al., 2012). Furthermore, 1,2,4,5-B4CA is the only B4CA that is commercially  
168 available as a standard, prohibiting the confident conversion of the absorption signal at 240 nm  
169 for the other B4CAs to quantities. Therefore, as in a previous study (Stubbins et al., 2012), total  
170 DBC concentrations here were calculated directly from the robustly quantified B5CA and B6CA  
171 concentrations. An extensive BPCA data set collected for the Southern Ocean (Dittmar and  
172 Paeng, 2009), the Gulf of Mexico (Dittmar et al., 2012b) and other regions (unpublished) was  
173 used to develop a power-function relationship ( $R = 0.998$ ,  $n = 351$ ,  $p < 0.0001$ ; Figure on Data

174 Sheet S1) to predict the concentration of DBC from the sum of the quantitatively dominant and  
175 robustly quantified B5CA and B6CA. This extrapolation reduced the analytical error range of  
176 replicate analysis for the calculation of total DBC within the model dataset to below 2% and  
177 provided a method to compare the data reported here with the total DBC concentrations reported  
178 elsewhere (Dittmar, 2008; Dittmar and Paeng, 2009; Dittmar et al., 2012a; Jaffé et al., 2013).

179 Given the differences in oxidation conditions and conversion factors applied in the  
180 literature, we also report the concentrations of the individual BPCAs to enable comparison with  
181 other datasets (Table S1).

### 182 3. Results

183 The six rivers were sampled at variable discharge (Table S1). Concentrations of DOC  
184 ranged from 2.6 to 17.5 mg-C L<sup>-1</sup>, and  $a_{254}$  from 12 to 148 m<sup>-1</sup>. Concentrations of each BPCA  
185 quantified are listed in Table S1. B5CA was the most abundant BPCA and total DBC  
186 concentrations ranged from 0.14 to 1.51 mg-C L<sup>-1</sup>. Changes in the quality of DBC being  
187 exported were also evident, with the B6CA:B5CA ratio ranging from 0.16 to 0.43 (Table S1).  
188 DBC loads on days when DBC concentrations were measured (i.e. DBC concentration × daily  
189 discharge) varied from 0.26 to 194.5 kg sec<sup>-1</sup> (Table S1). Within each river, the concentrations  
190 and loads of DBC were highest during peak discharge.

### 191 4. Discussion

#### 192 4.1 Dissolved black carbon concentrations

193 DBC concentrations varied by over an order of magnitude, from 0.14 to 1.51 mg-C L<sup>-1</sup>  
194 (Table S1). For comparison, reported DBC concentrations ranged from 0.002 to 2.77 mg-C L<sup>-1</sup> in  
195 global rivers (Jaffé et al., 2013) and from 0.02 to 0.88 mg-C L<sup>-1</sup> in a small Arctic stream  
196 (Guggenberger et al., 2008). Upper limits to the concentrations of highly bio-labile forms of  
197 thermogenic DOC have been estimated in the Siberian rivers studied here based upon  
198 concentrations of levoglucosan (Myers-Pigg et al., 2015). These highly bio-labile forms of  
199 thermogenic contribute up to 0.1 to 0.3 mg-C L<sup>-1</sup> to the DOC pool at the sites studied here (data  
200 from 2004-2006) (Myers-Pigg et al., 2015).

201 Previous work in the Arctic has demonstrated a strong link between DOC concentration  
202 and river hydrology. Early in the year, under ice flow cannot access the organic-rich seasonally  
203 thawed soil layer. Consequently, DOC concentrations in the river are low and sourced from  
204 groundwater (Table S1) (Holmes et al., 2012). In the spring, soils and waterways thaw, and the  
205 spring freshet inundates the watershed. DOC concentrations reach maxima during this flushing  
206 event and subsequently decline as water levels fall (Holmes et al., 2012). For DBC, the same  
207 trend of high concentration at high flow, is apparent in the regression of DBC concentrations  
208 versus runoff (watershed area normalized discharge; m<sup>3</sup> km<sup>-2</sup> sec<sup>-1</sup>; Table S1), which reveals a  
209 significant linear correlation across the 6 rivers studied (Figure 2A; R<sup>2</sup> = 0.63; n = 25; p  
210 <0.0001).

211 Plots of solute concentration versus runoff are used in hydrological studies to learn more  
212 about potential solute sources and the mechanisms controlling their export (Evans and Davies,  
213 1998). The simplest interpretation of the linear correlation between DBC and runoff requires the  
214 conservative mixing of only two sources. In the Paraíba do Sul River, Brazil, variations in DBC  
215 concentrations with hydrology were explained by a simple two endmember model, with low  
216 DBC concentrations in groundwater under base flow conditions mixing with inputs of higher, but



217 constant DBC concentration waters from active soil layers as discharge increased (Dittmar et al.,  
218 2012a). In Arctic rivers, the relationship between hydrology and DBC concentration also  
219 indicates that in the winter, when the watersheds are frozen and discharge at a minimum, rivers  
220 are dominated by inputs from groundwater with low DBC. As runoff increases in the spring, the  
221 hydrological pathway incorporates soil active layers, which are rich in organics, including  
222 soluble BC (Guggenberger et al., 2008).

223 The lack of a plateau at high runoff in the current dataset (Figure 2A) suggests that if runoff  
224 were to increase, then DBC concentrations would also continue to increase, leading to greater  
225 DBC export. Eurasian Arctic river discharge has increased (Peterson et al., 2002). Modelling  
226 studies predict that runoff will increase further as the Arctic warms in the future, with the  
227 greatest increases occurring as an amplification of the spring freshet (Van Vliet et al., 2013). If  
228 these models are correct, Figure 2A suggests DBC exports will also increase, with the spring  
229 freshet contributing ever more to annual DBC loads. Thus, both the magnitude and the timing of  
230 DBC delivery to the Arctic Ocean are liable to change in the future.

#### 231 **4.2 Dissolved black carbon quality**

232 The molecular BPCA method as applied here quantifies broad classes of DBC oxidation  
233 products, each with a different number of carboxylic groups (Dittmar, 2008). These are the:  
234 benzeneTRICarboxylic acids (B3); benzeneTETRAcarboxylic acids (B4);  
235 benzenePENTAcid (B5); and, benzeneHEXAcid (B6). Each of these  
236 BPCAs provides structural information about DBC. B6 is indicative of highly condensed  
237 aromatics, whereas the benzene products with lower numbers of carboxylic substitutes are  
238 indicative of molecules with smaller numbers of condensed rings at their core (Schneider et al.,  
239 2010). As B6 and B5 were the most robustly quantified BPCAs, only the ratios of these two  
240 BPCAs are reported. The B6:B5 ratio provides an index, where higher values indicate greater  
241 levels of the most condensed forms of DBC (Stubbins et al., 2012). B6:B5 ratios have been  
242 reported for Little Grawijka Creek, a small Arctic stream (watershed area 0.44 km<sup>2</sup>)  
243 (Guggenberger et al., 2008) within the watershed of the Yenisei River (watershed area 2.54×10<sup>6</sup>  
244 km<sup>2</sup>; Table 1). Comparison of B6:B5 values for the 6 large Arctic rivers (0.16 to 0.43; Table S1)  
245 to values in the Little Grawijka Creek (0.30 to 0.65) (Guggenberger et al., 2008) suggests the  
246 DBC within the mainstems of the large Arctic rivers may be less condensed than DBC in Little  
247 Grawijka Creek, and possibly other Arctic headwaters.

248 In the Siberian rivers (Kolyma, Lena, Ob' and Yenisey), there was a significant correlation  
249 between B6:B5 and runoff (Figure 2B). The logarithmic fit indicates that at low flow, these  
250 Siberian rivers are dominated by water from a source with low concentrations of DBC (Figure  
251 2A) and that the DBC in this water is less condensed than the DBC exported at high runoff  
252 (Figure 2B). The B6:B5 ratio then approaches a plateau at high runoff, where the value reached  
253 at the plateau can be considered the B6:B5 ratio of a putative high runoff, high DBC  
254 concentration endmember derived from the soil active layer. The logarithmic fit to the data  
255 (Figure 2B caption) suggests this endmember would have a B6:B5 ratio of 0.63, a value similar  
256 to the highest B6:B5 ratio observed at peak discharge during the spring freshet within Little  
257 Grawijka Creek (0.65) (Guggenberger et al., 2008).

258 Although future work is required to determine the source of DBC to Arctic rivers, in the  
259 current study, both the concentrations (Figure 2A) and the degree of DBC condensation (Figure  
260 2B) were elevated in the Siberian rivers during high flow, suggesting a soil source. It is unclear  
261 why this trend in B6:B5 was not apparent in the Yukon and Mackenzie Rivers of Northern  
262 America. The significantly higher sediment loads and associated sorption reactions in the North

263 American rivers (Holmes et al., 2012) may differentiate their B6:B5 ratios from those observed  
264 in the sediment-poor Siberian rivers. Within the Mackenzie, B6:B5 ratios may also be influenced  
265 by inputs from petrogenic sources (Yunker et al., 2002). More data is required to verify these  
266 trends and, once verified, to seek mechanistic explanations.

#### 267 **4.3 Estimating dissolved black carbon export from dissolved organic carbon**

268 DBC and DOC concentrations were correlated ( $R^2 = 0.96$ ; Figure 3A). Previous work has  
269 reported similar correlations between total DOC and DBC concentrations within rivers. For  
270 instance, Jaffe *et al.* (2013) conducted an assessment including 109 DBC concentrations for  
271 rivers diverse in stream order and latitude, including seasonally averaged values for the DBC  
272 values of the 6 Arctic rivers studied here (i.e. data for each of the 25 samples analyzed here were  
273 not presented in Jaffe *et al.* (2013), only their averages on a river-by-river basis). As in the  
274 current study, the intercept of the slope between DBC and DOC was statistically  
275 indistinguishable from zero (current study intercept =  $-0.019 \pm 0.035 \text{ mg-C L}^{-1}$ ). Therefore, Jaffe  
276 *et al.* (2013) interpreted the slope of the linear regression to approximate the globally averaged  
277 contribution of DBC to riverine DOC concentrations. For their dataset, DBC was estimated to  
278 account for  $10.5 \pm 0.7\%$  of global DOC exports. Following the same approach, reference to the  
279 slope in Figure 3A indicates that DBC constitutes  $8.9 \pm 0.3\%$  of Arctic river DOC. This suggests  
280 Arctic river DOC is slightly depleted in DBC relative to rivers globally, though larger datasets  
281 for both global and Arctic rivers are required to strengthen this conclusion. Jaffe *et al.* (2012)  
282 used the percentage contribution of DBC to riverine DOC concentrations and a global DOC load  
283 of  $250 \text{ Tg-C yr}^{-1}$  (Hedges et al., 1997) to estimate that  $26.5 \pm 0.8 \text{ Tg-C yr}^{-1}$  of DBC is exported to  
284 the oceans each year. An analogous calculation based upon an Arctic DOC load of  $34 \text{ Tg-C yr}^{-1}$   
285 (Holmes et al., 2012) and the DBC percentage for Arctic rivers, leads to an estimated DBC  
286 export by Arctic rivers of  $3.0 \pm 0.1 \text{ Tg-C yr}^{-1}$ .

#### 287 **4.4 Refining estimates of dissolved black carbon export using CDOM**

288 The above correlations between DOC and DBC provide a method of converting between  
289 relatively common DOC loads and rarer, more analytically challenging measurements of DBC.  
290 However, when looking for a proxy of aromatic carbon components, CDOM measurements offer  
291 even greater potential. First of all, light absorption by CDOM provides a robust empirical proxy  
292 for aromatic DOM components in Arctic rivers (Spencer et al., 2009) and model systems  
293 (Weishaar et al., 2003; Stubbins et al., 2008), including DBC concentrations in a photochemical  
294 degradation experiment (Stubbins et al., 2012). Second, measuring CDOM is simpler and  
295 cheaper than measuring DOC. Finally, estimates of CDOM can be made in situ with in water  
296 spectrophotometers (Spencer et al., 2007; Tait et al., 2015) and from space, using satellite remote  
297 sensing of water color (Griffin et al., 2011). To determine if CDOM could provide a robust  
298 proxy for DBC in Arctic rivers, a series of linear regressions were performed between DBC  
299 concentration and CDOM light absorption at wavelengths from 250 to 600 nm. Plotting the  
300 resultant correlation values (R) for the linear regressions against wavelength revealed which  
301 wavelengths provided the most robust proxies for DBC concentration (Figure 3B). Values for R  
302 peaked ( $R = 0.986$ ) around 254 nm, a wavelength long used to estimate the relative aromatic  
303 content of DOM (Weishaar et al., 2003). At longer wavelengths, R declined gradually to 0.971 at  
304 412 nm and 0.905 at 500 nm, before dropping more rapidly at increasing wavelengths (Figure  
305 3B). The robust correlation at 412 nm is encouraging for those wishing to remote sense DBC  
306 from space, as estimates of CDOM at 412 nm can be retrieved from SeaWiFS  
307 (<http://oceancolor.gsfc.nasa.gov/SeaWiFS>) and MODIS (<http://modis.gsfc.nasa.gov>) satellites.

308 In the current study, the equation of the linear regression between DBC and CDOM light  
309 absorption at 254 nm ( $a_{254}$ ) was used as a proxy to estimate DBC concentrations for each of the  
310 410 samples analyzed for CDOM (Figure 3C). This increased the temporal extent and resolution  
311 of our DBC dataset from 25 samples over 1 year to 410 samples over 7 years. Under ice  
312 sampling for CDOM was limited as it is logistically challenging. Where data gaps exceeding one  
313 month occurred, the average under ice CDOM for each river was used to estimate winter  
314 concentrations of DBC for the modelling exercise below. This is unlikely to have significantly  
315 altered estimates of DBC export as under ice DOC concentration and water discharge are low  
316 and contribute minimally to annual Arctic river discharge and DOC loads (Holmes et al., 2012).

#### 317 **4.5 LOADEST model estimates of daily dissolved black carbon loads**

318 The goal of the current study was to develop a continuous recorded of DBC export for each  
319 river across 7 years. To achieve this, daily discharge values for each river, along with the 410  
320 CDOM derived DBC concentrations, were entered into a hydrological load estimating model  
321 (LOADEST using predefined regression model 4; <http://water.usgs.gov/software/loadest>)  
322 (Runkel et al., 2004) to determine daily and annual DBC loads. The predefined model 4 was  
323 chosen as it provides robust estimates of DOC export for Arctic rivers and to enable the resultant  
324 DBC loads to be compared directly to previous estimates of DOC loads made using the same  
325 model (Holmes et al., 2012). Output from the model provides estimated daily loads for DBC  
326 across the 7 years of hydrological data. To assess model performance, modelled daily loads were  
327 compared to daily loads calculated for the 25 days when DBC samples were collected. On these  
328 days, DBC loads were calculated as DBC concentration multiplied by measured discharge at the  
329 gauging station (Table S1). The hydrograph together with predicted and measured DBC loads for  
330 the Lena River are presented in Figure 4. Visual inspection indicates the model matches  
331 calculated data. Considering data for all rivers, the mean absolute error between modelled and  
332 calculated DBC loads was 11%. A two component linear regression ( $R^2 = 0.987$ ;  $p < 0.0001$ ) of  
333 modelled versus calculated DBC loads yielded a slope of  $0.999 \pm 0.02$  ( $p < 0.0001$ ) and intercept  
334 of  $0.11 \pm 0.11$  ( $p = 0.3489$ ). The intercept was insignificantly different from zero. Forcing the  
335 slope through zero yielded a slope of  $1.01 \pm 0.02$  ( $R^2 = 0.987$ ;  $p < 0.0001$ ; Figure 5). That the  
336 slope of the regression was insignificantly different from unity (i.e. 1) indicates that use of  $a_{254}$   
337 as a proxy for DBC and the assumptions of the LOADEST model provided a quantitatively  
338 robust estimate of daily DBC loads.

339 Gauging stations were near the mouths of the rivers, capturing from 82 to 100 % of each  
340 individual river's discharge, and 96% of the six rivers' combined discharge (Table 1). To  
341 determine DBC loads ( $Gg-C yr^{-1}$ ) for the entirety of the river watersheds, the DBC yields ( $Gg-C$   
342  $km^{-2} yr^{-1}$ ) for the gauged river areas were extrapolated to the total river area (Table 1). The same  
343 modeling exercise was repeated for each BPCA quantified. Annual export of each BPCA to the  
344 Arctic Ocean is presented in the Supplemental Information (Tables S2A-D). Below we focus  
345 upon the total DBC flux estimates.

346 The annual DBC load for the six rivers ranged from 1.4 million tons per year in 2004 and  
347 2010 to 1.7 million tons per year in 2007. Interannual variations in DBC loads were greater than  
348 interannual variation in discharge, highlighting how variations in discharge amplify variations in  
349 the export of dissolved organics (compare Table 1 and Table 2). The greatest year-to-year  
350 variation was observed in the Kolyma (33% st. dev.) and the Yukon (27% st. dev.) Rivers while  
351 the Yenisey River (5% st. dev.) showed the lowest interannual variation in loads (Table 2). The  
352 majority of the trend in interannual variability in DBC loads between rivers stems from their  
353 trends in interannual variability in discharge, which is also greatest in the Kolyma (20%) and

354 minimal in the Yenisey River (4%) (Table 1). However, interannual variability in the Yukon  
355 River discharge was only 12%, suggesting that Yukon River DBC export is particularly sensitive  
356 to discharge variation. The average annual DBC load for the six rivers was  $1.5 \pm 0.1$  million tons  
357 per year (Table 2). This translates to an average areal yield of  $138 \pm 13 \text{ kg-C km}^{-2} \text{ yr}^{-1}$ , a DBC  
358 yield similar to that determined for a tundra forest watershed in Northern Siberia ( $100 \text{ kg-C km}^{-2}$   
359  $\text{yr}^{-1}$ ) (Guggenberger et al., 2008), but more than double that of the Paraíba do Sul which drains  
360 an area of intense slash-and-burn land clearing in Brazil (Dittmar et al., 2012a).

361 The gauged area of the six rivers studied covered  $10.9 \times 10^6 \text{ km}^2$  or 53% of the pan-  
362 Arctic watershed (Figure 1). A pan-Arctic DBC load of  $2.8 \pm 0.25$  million tons per year was  
363 estimated assuming DBC yields to be the same in the sampled and unsampled fractions of the  
364 pan-Arctic watershed. Riverine export of particulate BC has been presented for the six rivers  
365 studied here (Elmquist et al., 2008) (Table 2). This estimate of particulate BC loads (Elmquist et  
366 al., 2008) was made using the chemothermic oxidation (CTO) method that over estimates BC in  
367 organic rich samples such as particulate organic matter samples (Hammes et al., 2007).  
368 Therefore, the particulate BC fluxes should be considered an upper limit or an over estimate of  
369 true loads. Despite the potential for the particulate BC to be an overestimate, the load of DBC  
370 from the six rivers is eight times that of particulate BC (Table 2). This makes riverine DBC  
371 export the largest quantified term for BC removal from the pan-Arctic watershed, suggesting that  
372 DBC export plays a major role in the Arctic storage of soil BC. This appears to be true elsewhere  
373 in the world. For instance, estimated DBC export by a tropical river in Brazil is far greater than  
374 contemporary BC production in the watershed (Dittmar et al., 2012a).

375 Comparing DBC export to total organic carbon fluxes reveals that DBC contributes  
376 approximately 8% of DOC export (Holmes et al., 2012), which is slightly less than the 8.9% of  
377 DOC estimated using the linear correlation between DBC and DOC (Figure 3A). This flux  
378 equates to 36% of total particulate organic carbon (POC) export from the six rivers studied (Stein  
379 and MacDonald, 2004) (Table 2). The export and burial of terrestrial POC in ocean margins is a  
380 significant long-term carbon sink (Blair and Aller, 2012). By analogy, if DBC is also locked  
381 away in the marine environment, riverine DBC export represents a translocation of refractory  
382 carbon from one store to another. If however, DBC is labile within the ocean, the once refractory  
383 carbon stored in the soil black carbon pool will re-enter the contemporary carbon cycle. As DBC  
384 is refractory in the deep ocean (Dittmar and Paeng, 2009; Ziolkowski and Druffel, 2010), yet  
385 highly labile when exposed to sunlight (Stubbins et al., 2010; Stubbins et al., 2012), the  
386 efficiency of carbon translocation from soil to ocean stores may be strongest in Arctic waters  
387 where it has been demonstrated that a significant fraction of other terrestrially derived, photo-  
388 labile aromatics survive transport to the major regions of North Atlantic Deep Water formation  
389 (Benner et al., 2005). Therefore, although Arctic rivers contribute 11% of the 26.5 million tons  
390 per year of DBC delivered to the oceans globally (Jaffé et al., 2013), their relative contribution to  
391 the global deep ocean store of DBC is potentially much higher. The Arctic rivers alone would  
392 replenish the global marine pool of DBC ( $>12 \text{ Pg-C}$ ) (Dittmar and Paeng, 2009) in  
393 approximately 4,300 years. This initial estimate is considerably shorter than the apparent age of  
394 DBC in the open ocean (Ziolkowski and Druffel, 2010) suggesting that Arctic river DBC export  
395 and subsequent entrainment into the abyssal ocean at points of deep water formation could  
396 provide the single most important pathway of DBC delivery to the deep ocean.

## 397 **5. Conclusions**

398 Today, the DBC mediated transfer of BC from the land to the oceans is a major term in  
399 the Arctic carbon cycle. In terms of continued research, measurement of photo-labile, but bio-  
400 refractory thermogenic DOM, i.e. DBC quantified as BPCAs, and highly bio-labile thermogenic  
401 DOM quantified via levoglucosan offer an intriguing dual tracer approach to assess the dynamics  
402 of thermogenic DOM within aquatic systems {Myers-Pigg, 2015 #2367}. Optical measurements  
403 of absorbance, including at 412 nm, a wavelength amenable to remote sensing, provide robust  
404 proxies for DBC concentrations in Arctic rivers that should enable us to resolve temporal and  
405 spatial patterns in DBC cycling. Looking to the future of the Arctic, Arctic warming is set to  
406 continue at rates exceeding global average temperature increases, leading to pronounced  
407 perturbations in the Arctic which are likely to increase the production and export of BC.  
408 Warming and associated changes to the water cycle appear to be increasing Arctic wildfire  
409 frequency (Higuera et al., 2008;Hu et al., 2010), potentially increasing BC production. Arctic  
410 soils store the largest pool of organic carbon on the planet (Gruber et al., 2004). Changing  
411 climate in the Arctic is increasing river water discharge (Peterson et al., 2002;Van Vliet et al.,  
412 2013). Increasing runoff will likely increase DBC export (Figure 2). Therefore, it is likely that  
413 the transfer of BC from Arctic soils to the deep ocean will accelerate. Measurements of CDOM  
414 light absorption for discrete water samples, using in situ spectrophotometers, or via remote  
415 sensing techniques could provide an effective way of monitoring future DBC fluxes to the  
416 Arctic, so long as periodic checks are made to test the continuing veracity of the linear regression  
417 presented here (Figure 3C). The eventual fate of exported DBC in the Arctic and global ocean  
418 will influence the sign and degree of climate-carbon cycle feedbacks. If exported DBC is  
419 effectively photo-degraded in ocean surface waters, its carbon will likely enter the atmospheric  
420 CO<sub>2</sub> pool. However, if exported Arctic DBC reaches areas of deep water formation around  
421 Greenland, it will be reburied, not in the soils of the Arctic, but the deep waters of the global  
422 ocean.  
423

424 **6.Acknowledgments**

425 Ekaterina Bulygina is thanked for CDOM analyses, Ina Ulber for assistance with BPCA samples,  
426 Greg Fiske for assistance with GIS analysis and the preparation of Figure 1, and Anna Boyette  
427 for assistance with figures. This work was funded by the U.S. National Science Foundation  
428 (ANT-1203885, OPP-0732522, OPP-0732821, OPP-1107774, DEB-1146161, DEB-1145932,  
429 PLR-1500169) and a Fellowship from the Hanse Institute for Advanced Studies (HWK,  
430 Delmenhorst, Germany) granted to AS. Data are archived at the Skidaway Institute of  
431 Oceanography and are attainable from AS or via the Arctic Great Rivers Observatory website  
432 (<http://arcticgreatrivers.org/>).

433

434

435

In review

436 **Figure 1.** Map showing the six Arctic river watersheds sampled. The red dots indicate the  
437 sampling locations. Red line indicates the boundary and the grey fill the area of the pan-Arctic  
438 Ocean watershed. Data points in all subsequent figures are colored to match the river watershed  
439 colors here.

440 **Figure 2. Panel A: Dissolved black carbon concentrations ([DBC]) versus runoff for**  
441 **samples from across the hydrographs of the six Arctic rivers.** Black line represents the linear  
442 regression of the data ( $[DBC] \text{ mg-C L}^{-1} = 0.359 + 21.94 \times \text{runoff}$ ; Standard error of the intercept  
443  $= 0.075$ ; Standard error of the slope  $= 3.48$ ;  $R^2 = 0.63$ ;  $n = 25$ ;  $p < 0.0001$ ). Dark grey represents  
444 extent of the prediction of fit (95% confidence limit). Light grey represents extent of prediction  
445 of prediction (95% confidence limit). **Panel B: The ratio of benzeneHEXAcid to**  
446 **benzenePENTAcid (B6:B5) versus runoff for samples from across the**  
447 **hydrographs of the six Arctic rivers.** Data points from North American rivers are faded. Black  
448 line represents the logarithmic regression of the data from the Siberian rivers ( $B6:B5 = 0.638 +$   
449  $0.0683 \ln(\text{runoff})$ ; Standard error of the intercept  $= 0.033$ ; Standard error of the slope  $= 0.007$ ;  $R^2$   
450  $= 0.84$ ;  $p < 0.0001$ ;  $n = 18$ ).

451 **Figure 3. Panel A: Dissolved black carbon concentration ([DBC]) versus dissolved organic**  
452 **carbon concentration ([DOC]).** Black line represents the linear regression of the data ( $[DBC] =$   
453  $-0.019 + 0.887 \times [DOC]$ ; Standard error of the intercept  $= 0.035$ ; Standard error of the slope  $=$   
454  $0.004$ ;  $R^2 = 0.96$ ;  $n = 25$ ;  $p < 0.0001$ ). **Panel B: Plot of correlation coefficient (R) values for**  
455 **linear regressions of [DBC] versus colored dissolved organic carbon Naperian light**  
456 **absorption coefficients ( $a_{CDOM}$ ) versus wavelength. Panel C: [DBC] versus  $a_{CDOM}$  at**  
457 **254 nm ( $a_{254}$ ).** Black line represents the linear regression of the data ( $[DBC] = 0.104 + 0.00942$   
458  $\times a_{254}$ ; Standard error of the intercept  $= 0.028$ ; Standard error of the slope  $= 0.00036$ ;  $R = 0.986$ ;  
459  $R^2 = 0.968$ ;  $n = 25$ ;  $p < 0.0001$ ).

460 **Figure 4. Discharge plus calculated and modeled dissolved black carbon (DBC) loads for**  
461 **the Lena River between 2004 and 2010.** Loads calculated from measured DBC were calculated  
462 as discharge on the day DBC was sampled multiplied by the measured [DBC] ( $n = 5$ ). Loads  
463 calculated based upon colored dissolved organic matter (CDOM) derived DBC were calculated  
464 discharge on the days CDOM was sampled multiplied by [DBC] estimated from CDOM  
465 absorbance and the slope of the linear regression in Figure 3C ( $n = 132$ ). LOADEST modeled  
466 loads were estimated using the LOADEST load model with daily discharge and CDOM based  
467 estimates of [DBC] as input data ( $n = 2557$ ).

468 **Figure 5. LOADEST modeled dissolved black carbon (DBC) loads versus loads calculated**  
469 **from measured [DBC] and discharge on the day of sampling.** Black line represents the zero  
470 intercept linear regression of the data. When the fit was not constrained, the intercept was not  
471 significantly different from zero ( $0.11 \pm 0.11$ ;  $p = 0.35$ ). Therefore, the intercept was constrained  
472 to zero and the fit on the graph has the following parameters (LOADEST modeled load = Load  
473 calculated from measured [DBC]  $\times 1.012$ ;  $R^2 = 0.987$ ; Standard error of the slope  $= 0.019$ ;  $p$   
474  $< 0.0001$ ;  $n = 25$ ).

475  
476

477 **Table 1. Discharge gauging stations and watershed characteristics.**

478

River / Watershed	Kolyma	Lena	Mackenzie	Ob'	Yenisey	Yukon
Discharge gauging station	Kolymskoye	Kyusyur	Tsiigehtchic	Salekhard	Igarka	Pilot Station
Area (10 <sup>6</sup> km <sup>2</sup> ) at gauged	0.53	2.43	1.68	2.99	2.4	0.83
Area (10 <sup>6</sup> km <sup>2</sup> ) total	0.65	2.46	1.78	2.99	2.54	0.83
% Area captured	82%	99%	94%	100%	94%	100%
Discharge (km <sup>3</sup> year <sup>-1</sup> ) gauged	111	581	298	427	636	208
Discharge (km <sup>3</sup> year <sup>-1</sup> ) total	136	588	316	427	673	208
Interannual variation in discharge (St. Dev.)	20%	9%	10%	15%	4%	12%
Runoff (mm year <sup>-1</sup> )	166	240	177	143	259	248

479

480

481

482

In review



483 **Table 2.** Average dissolved black carbon (DBC) loads, yields and interannual variation in both  
 484 for the six rivers studied and for the pan-Arctic watershed, plus literature values for the rivers'  
 485 dissolved organic carbon (DOC) (Holmes et al., 2012), particulate organic carbon (POC) (Stein  
 486 and MacDonald, 2004) and particulate black carbon (PBC) (Elmqvist et al., 2008) loads.

487

River / Watershed	DBC load (Gg-C yr <sup>-1</sup> )	DBC yield (kg-C km <sup>-2</sup> yr <sup>-1</sup> )	Interannual variation (St. Dev.)	DOC load (Gg-C yr <sup>-1</sup> )	PBC load (Gg-C yr <sup>-1</sup> )	POC load (Gg-C yr <sup>-1</sup> )
Kolyma	62±20	116±38	33%	818	24	310
Lena	550±68	226±28	16%	5,681	36	1,200
Mackenzie	129±20	77±12	12%	1,377	99	2,100
Ob'	262±44	87±15	17%	4,119	18	360
Yenisey	402±19	167±8	5%	4,645	10	170
Yukon	102±28	123±34	27%	1,472	1.1	12
Total for six rivers	1,506±133	138±13	-	18,109	188	4,152
Pan-Arctic	2,842±250	-	-	34,042	-	-

488

489

490 References

- 491
- 492 Benner, R., Louchouart, P., and Amon, R.M. (2005). Terrigenous dissolved organic matter in the Arctic Ocean and  
 493 its transport to surface and deep waters of the North Atlantic. *Global Biogeochemical Cycles* 19.
- 494 Blair, N.E., and Aller, R.C. (2012). The fate of terrestrial organic carbon in the marine environment. *Annual Review*  
 495 *of Marine Science* 4, 401-423.
- 496 Bowman, D.M.J.S., Balch, J.K., Artaxo, P., Bond, W.J., Carlson, J.M., Cochrane, M.A., D'antonio, C.M., Defries,  
 497 R.S., Doyle, J.C., Harrison, S.P., Johnston, F.H., Keeley, J.E., Krawchuk, M.A., Kull, C.A., Marston, J.B.,  
 498 Moritz, M.A., Prentice, I.C., Roos, C.I., Scott, A.C., Swetnam, T.W., Van Der Werf, G.R., and Pyne, S.J.  
 499 (2009). Fire in the earth system. *Science* 324, 481-484.
- 500 Dittmar, T. (2008). The molecular level determination of black carbon in marine dissolved organic matter. *Organic*  
 501 *Geochemistry* 39, 396-407.
- 502 Dittmar, T., De Rezende, C.E., Manecki, M., Niggemann, J., Coelho Ovalle, A.R., Stubbins, A., and Bernardes,  
 503 M.C. (2012a). Continuous flux of dissolved black carbon from a vanished tropical forest biome. *Nature*  
 504 *Geoscience* 5, 618-622.
- 505 Dittmar, T., and Paeng, J. (2009). A heat-induced molecular signature in marine dissolved organic matter. *Nature*  
 506 *Geoscience* 2, 175-179.
- 507 Dittmar, T., Paeng, J., Gihring, T.M., Suryaputra, I.G., and Huettel, M. (2012b). Discharge of dissolved black  
 508 carbon from a fire-affected intertidal system. *Limnology and Oceanography* 57, 1171-1181.
- 509 Elmquist, M., Semiletov, I., Guo, L., and Gustafsson, Ö. (2008). Pan-Arctic patterns in black carbon sources and  
 510 fluvial discharges deduced from radiocarbon and PAH source apportionment markers in estuarine surface  
 511 sediments. *Global Biogeochemical Cycles* 22.
- 512 Evans, C., and Davies, T.D. (1998). Causes of concentration/discharge hysteresis and its potential as a tool for  
 513 analysis of episode hydrochemistry. *Water Resources Research* 34, 129-137.
- 514 Forbes, M.S., Raison, R.J., and Skjemstad, J.O. (2006). Formation, transformation and transport of black carbon  
 515 (charcoal) in terrestrial and aquatic ecosystems. *Science of the Total Environment* 370, 190-206.
- 516 Glaser, B., Haumaier, L., Guggenberger, G., and Zech, W. (1998). Black carbon in soils: The use of  
 517 benzenecarboxylic acids as specific markers. *Organic Geochemistry* 29, 811-819.
- 518 Griffin, C.G., Frey, K.E., Rogan, J., and Holmes, R.M. (2011). Spatial and interannual variability of dissolved  
 519 organic matter in the Kolyma River, East Siberia, observed using satellite imagery. *Journal of Geophysical*  
 520 *Research: Biogeosciences (2005–2012)* 116.
- 521 Gruber, N., Friedlingstein, P., Field, C.B., Valentini, R., Heimann, M., Richey, J.E., Lankao, P.R., Schulze, E.-D.,  
 522 and Chen, C.-T.A. (2004). The vulnerability of the carbon cycle in the 21st century: An assessment of  
 523 carbon-climate-human interactions. *Scope-Scientific committee on problems of the environment*  
 524 *international council of scientific unions* 62, 45-76.
- 525 Guggenberger, G., Rodionov, A., Shibistova, O., Grabe, M., Kasansky, O.A., Fuchs, H., Mikheyeva, N.,  
 526 Zrazhevskaya, G., and Flessa, H. (2008). Storage and mobility of black carbon in permafrost soils of the  
 527 forest tundra ecotone in Northern Siberia. *Global Change Biology* 14, 1367-1381.
- 528 Hammes, K., Schmidt, M.W.I., Smernik, R.J., Currie, L.A., Ball, W.P., Nguyen, T.H., Louchouart, P., Houel, S.,  
 529 Gustafsson, Ö., Elmquist, M., Cornelissen, G., Skjemstad, J.O., Masiello, C.A., Song, J., Peng, P., Mitra,  
 530 S., Dunn, J.C., Hatcher, P.G., Hockaday, W.C., Smith, D.M., Hartkopf-Fröder, C., Böhmer, A., Lüer, B.,  
 531 Huebert, B.J., Amelung, W., Brodowski, S., Huang, L., Zhang, W., Gschwend, P.M., Flores-Cervantes,  
 532 D.X., Largeau, C., Rouzaud, J.N., Rumpel, C., Guggenberger, G., Kaiser, K., Rodionov, A., Gonzalez-Vila,  
 533 F.J., Gonzalez-Perez, J.S., De La Rosa, J.M., Manning, D.a.C., López-Capél, E., and Ding, L. (2007).  
 534 Comparison of quantification methods to measure fire-derived (black-elemental) carbon in soils and  
 535 sediments using reference materials from soil, water, sediment and the atmosphere. *Global Biogeochemical*  
 536 *Cycles* 21.
- 537 Hansell, D.A. (2013). Recalcitrant dissolved organic carbon fractions. *Annual Review of Marine Science* 5, 421-445.
- 538 Hedges, J., Keil, R., and Benner, R. (1997). What happens to terrestrial organic matter in the ocean? *Organic*  
 539 *geochemistry* 27, 195-212.
- 540 Higuera, P.E., Brubaker, L.B., Anderson, P.M., Brown, T.A., Kennedy, A.T., and Hu, F.S. (2008). Frequent fires in  
 541 ancient shrub tundra: implications of paleorecords for arctic environmental change. *PLoS One* 3, e0001744.
- 542 Holmes, R.M., McClelland, J.W., Peterson, B.J., Tank, S.E., Buluygina, E., Eglinton, T.I., Gordeev, V.V., Gurtovaya,  
 543 T.Y., Raymond, P.A., Repeta, D.J., Staples, R., Striegl, R.G., Zhulidov, A.V., and Zimov, S.A. (2012).

544 Seasonal and Annual Fluxes of Nutrients and Organic Matter from Large Rivers to the Arctic Ocean and  
545 Surrounding Seas. *Estuaries and Coasts* 35, 369-382.

546 Hu, C., Muller-Karger, F.E., and Zepp, R.G. (2002). Absorbance, absorption coefficient, and apparent quantum  
547 yield: A comment on common ambiguity in the use of these optical concepts. *Limnology and*  
548 *Oceanography* 47, 1261-1267.

549 Hu, F.S., Higuera, P.E., Walsh, J.E., Chapman, W.L., Duffy, P.A., Brubaker, L.B., and Chipman, M.L. (2010).  
550 Tundra burning in Alaska: linkages to climatic change and sea ice retreat. *Journal of Geophysical*  
551 *Research: Biogeosciences (2005–2012)* 115.

552 Jaffé, R., Ding, Y., Niggemann, J., Vähätalo, A.V., Stubbins, A., Spencer, R.G.M., Campbell, J., and Dittmar, T.  
553 (2013). Global charcoal mobilization from soils via dissolution and riverine transport to the oceans. *Science*  
554 340, 345-347.

555 Jurado, E., Dachs, J., Duarte, C.M., and Simo, R. (2008). Atmospheric deposition of organic and black carbon to the  
556 global oceans. *Atmospheric Environment* 42, 7931-7939.

557 Mitra, S., Zimmerman, A., Hunsinger, G., and Woerner, W. (2013). Black carbon in coastal and large river systems.  
558 *Biogeochemical Dynamics at Major River-Coastal Interfaces: Linkages With Global Change* 200, 200-236.

559 Myers-Pigg, A.N., Louchouart, P., Amon, R.M., Prokushkin, A., Pierce, K., and Rubtsov, A. (2015). Labile  
560 pyrogenic dissolved organic carbon in major Siberian Arctic rivers: Implications for wildfire-stream  
561 metabolic linkages. *Geophysical Research Letters* 42, 377-385.

562 Peterson, B.J., Holmes, R.M., McClelland, J.W., Vörösmarty, C.J., Lammers, R.B., Shiklomanov, A.I.,  
563 Shiklomanov, I.A., and Rahmstorf, S. (2002). Increasing river discharge to the Arctic Ocean. *science* 298,  
564 2171-2173.

565 Raymond, P.A., McClelland, J.W., Holmes, R.M., Zhulidov, A.V., Mull, K., Peterson, B.J., Striegl, R.G., Aiken,  
566 G.R., and Gurtovaya, T.Y. (2007). Flux and age of dissolved organic carbon exported to the Arctic Ocean:  
567 A carbon isotopic study of the five largest arctic rivers. *Global Biogeochemical Cycles* 21.

568 Runkel, R.L., Crawford, C.G., and Cohn, T.A. (2004). "Load Estimator (LOADEST): A FORTRAN program for  
569 estimating constituent loads in streams and rivers".

570 Schmidt, M.W.I., Torn, M.S., Abiven, S., Dittmar, T., Guggenberger, G., Janssens, I.A., Kleber, M., Kögel-  
571 Knabner, I., Lehmann, J., Manning, D.a.C., Nannipieri, P., Rasse, D.P., Weiner, S., and Trumbore, S.E.  
572 (2011). Persistence of soil organic matter as an ecosystem property. *Nature* 478, 49-56.

573 Schneider, M.P.W., Hilf, M., Vogt, U.F., and Schmidt, M.W.I. (2010). The benzene polycarboxylic acid (BPCA)  
574 pattern of wood pyrolyzed between 200°C and 1000°C. *Organic Geochemistry* 41, 1082-1088.

575 Spencer, R.G.M., Aiken, G.R., Butler, K.D., Dornblaser, M.M., Striegl, R.G., and Hernes, P.J. (2009). Utilizing  
576 chromophoric dissolved organic matter measurements to derive export and reactivity of dissolved organic  
577 carbon exported to the Arctic Ocean: A case study of the Yukon River, Alaska. *Geophysical Research*  
578 *Letters* 36.

579 Spencer, R.G.M., Pellerin, B.A., Bergamaschi, B.A., Downing, B.D., Kraus, T.E.C., Smart, D.R., Dahlgren, R.A.,  
580 and Hernes, P.J. (2007). Diurnal variability in riverine dissolved organic matter composition determined by  
581 in situ optical measurement in the San Joaquin River (California, USA). *Hydrological Processes* 21, 3181-  
582 3189.

583 Stein, R., and Macdonald, R.W. (2004). *The organic carbon cycle in the Arctic Ocean*. Springer.

584 Stubbins, A., and Dittmar, T. (2012). Low volume quantification of dissolved organic carbon and dissolved  
585 nitrogen. *Limnology and Oceanography: Methods* 10, 347-352.

586 Stubbins, A., Hubbard, V., Uher, G., Law, C.S., Upstill-Goddard, R.C., Aiken, G.R., and Kenneth, M. (2008).  
587 Relating carbon monoxide photoproduction to dissolved organic matter functionality. *Environmental*  
588 *Science and Technology* 42, 3271-3276.

589 Stubbins, A., Law, C.S., Uher, G., and Upstill-Goddard, R.C. (2011). Carbon monoxide apparent quantum yields  
590 and photoproduction in the Tyne estuary. *Biogeosciences* 8, 703-713.

591 Stubbins, A., Niggemann, J., and Dittmar, T. (2012). Photo-lability of deep ocean dissolved black carbon.  
592 *Biogeosciences* 9, 1661-1670.

593 Stubbins, A., Spencer, R.G.M., Chen, H., Hatcher, P.G., Mopper, K., Hernes, P.J., Mwamba, V.L., Mangangu,  
594 A.M., Wabakanghanzi, J.N., and Six, J. (2010). Illuminated darkness: Molecular signatures of Congo River  
595 dissolved organic matter and its photochemical alteration as revealed by ultrahigh precision mass  
596 spectrometry. *Limnology and Oceanography* 55, 1467-1477.

597 Tait, Z.S., Thompson, M., and Stubbins, A. (2015). Chemical Fouling Reduction of a Submersible Steel  
598 Spectrophotometer in Estuarine Environments Using a Sacrificial Zinc Anode. *Journal of Environmental*  
599 *Quality*.

600 Van Vliet, M.T.H., Franssen, W.H.P., Yearsley, J.R., Ludwig, F., Haddeland, I., Lettenmaier, D.P., and Kabat, P.  
601 (2013). Global river discharge and water temperature under climate change. *Global Environmental Change*  
602 23, 450-464.

603 Weishaar, J.L., Aiken, G.R., Bergamaschi, B.A., Fram, M.S., Fujii, R., and Mopper, K. (2003). Evaluation of  
604 specific ultraviolet absorbance as an indicator of the chemical composition and reactivity of dissolved  
605 organic carbon. *Environmental Science and Technology* 37, 4702-4708.

606 Yunker, M., Backus, S., Pannatier, E.G., Jeffries, D., and Macdonald, R. (2002). Sources and significance of alkane  
607 and PAH hydrocarbons in Canadian arctic rivers. *Estuarine, Coastal and Shelf Science* 55, 1-31.

608 Ziolkowski, L.A., Chamberlin, A., Greaves, J., and Druffel, E.R. (2011). Quantification of black carbon in marine  
609 systems using the benzene polycarboxylic acid method: a mechanistic and yield study. *Limnology and*  
610 *Oceanography: Methods* 9, 140-140.

611 Ziolkowski, L.A., and Druffel, E.R.M. (2010). Aged black carbon identified in marine dissolved organic carbon.  
612 *Geophysical Research Letters* 37.

613

614

In review

Figure 1.JPEG

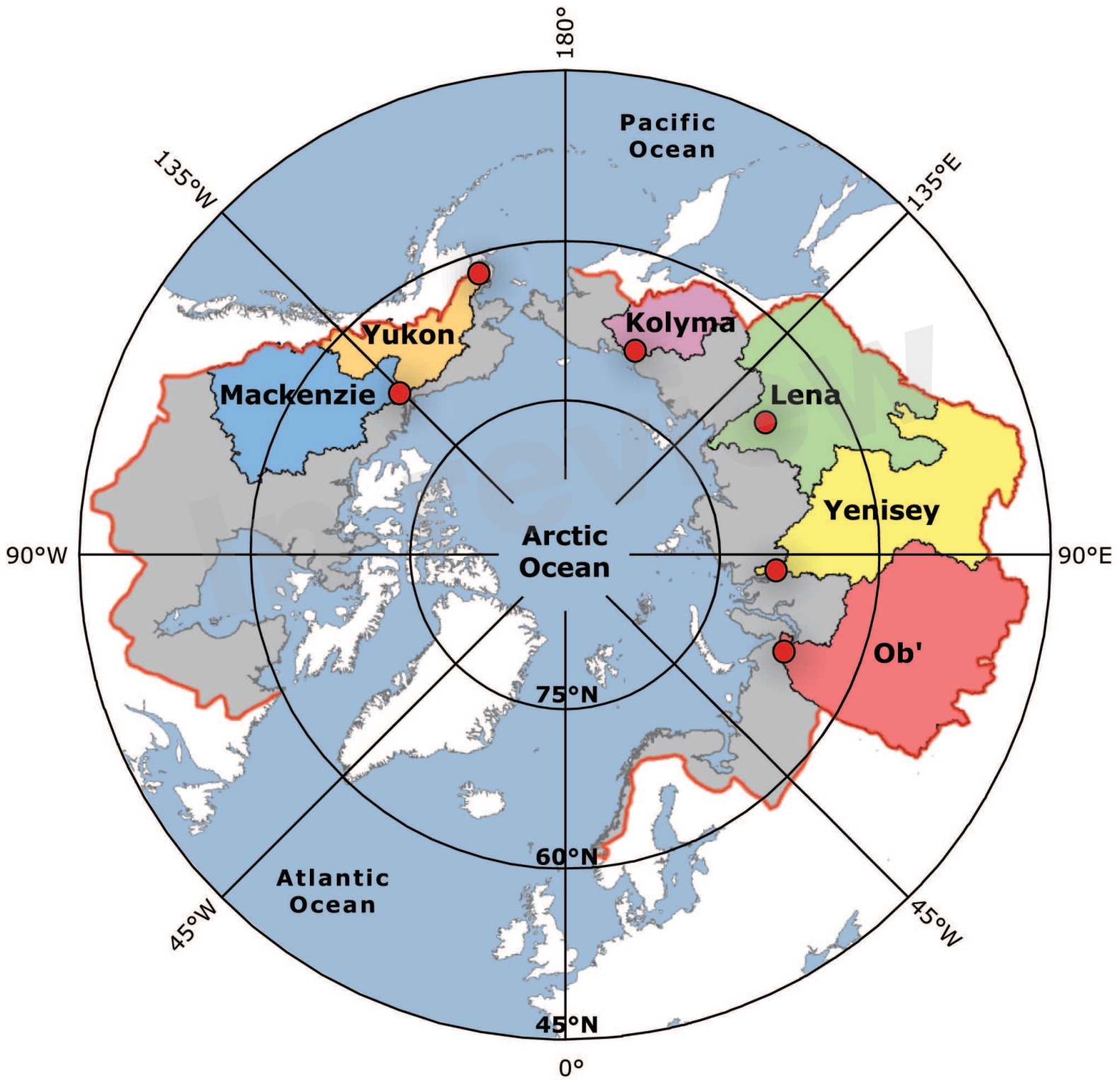
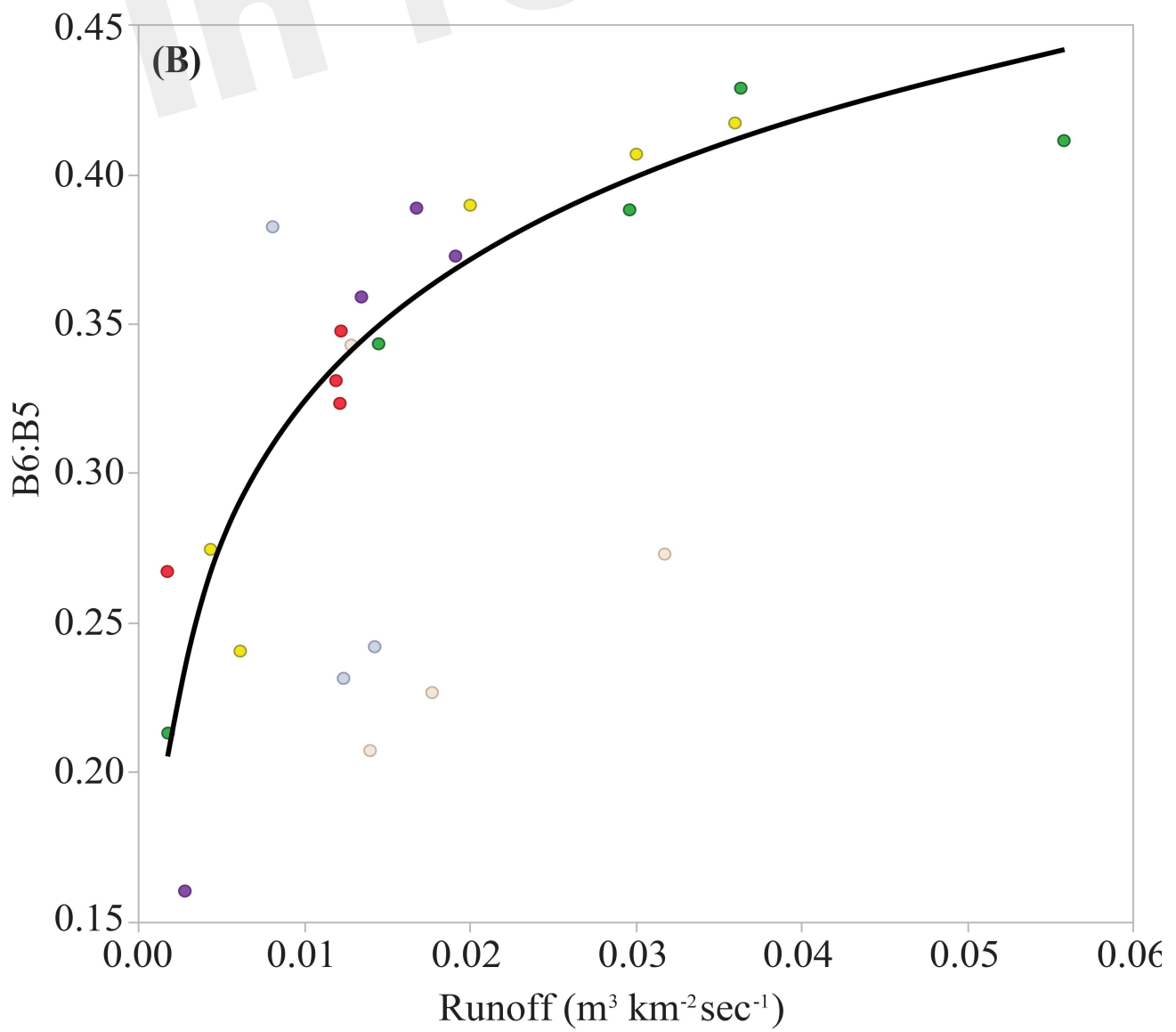
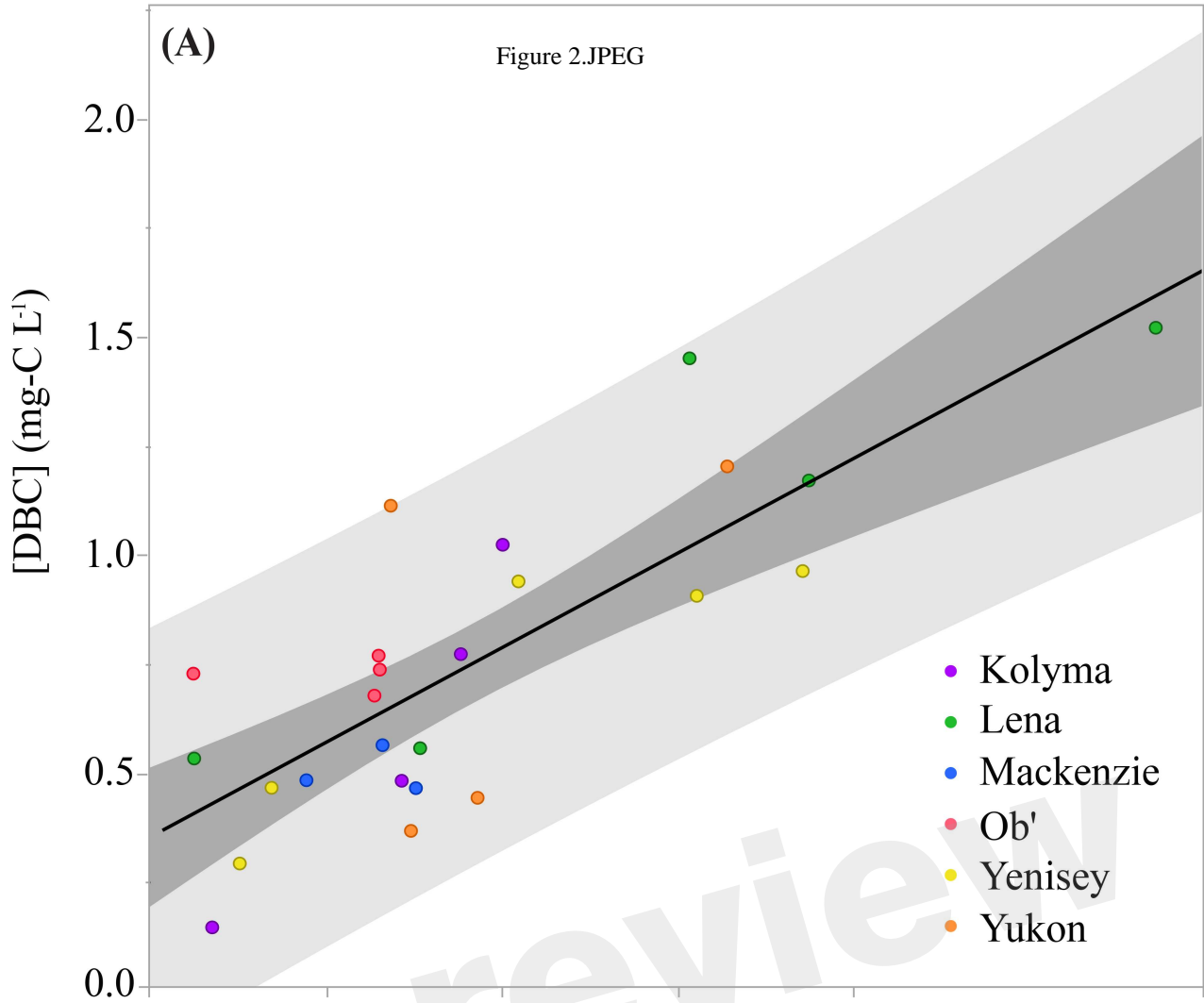


Figure 2.JPEG



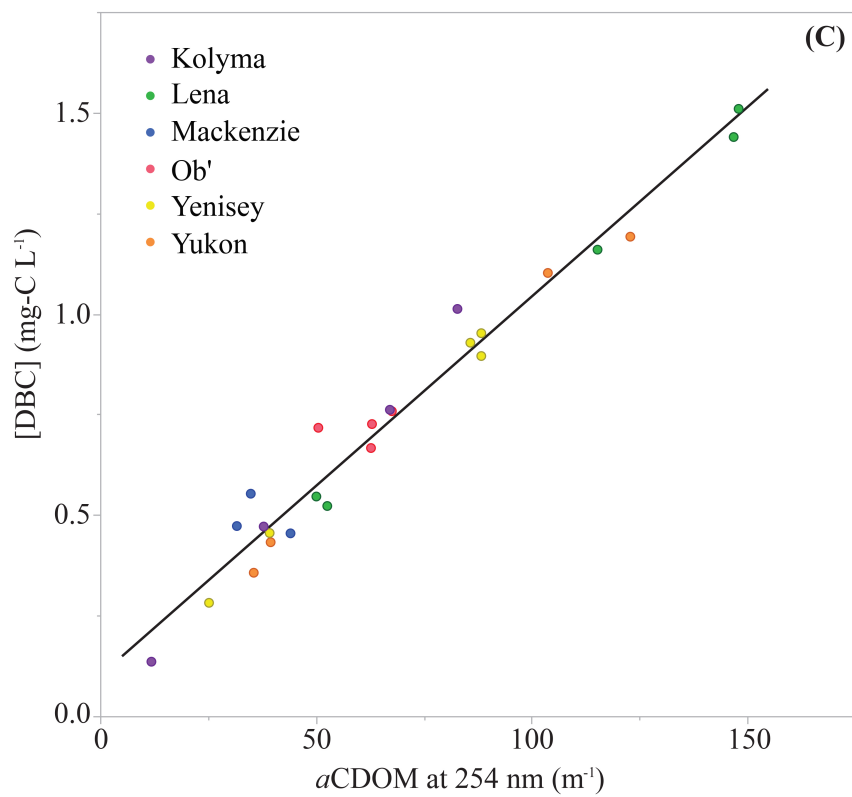
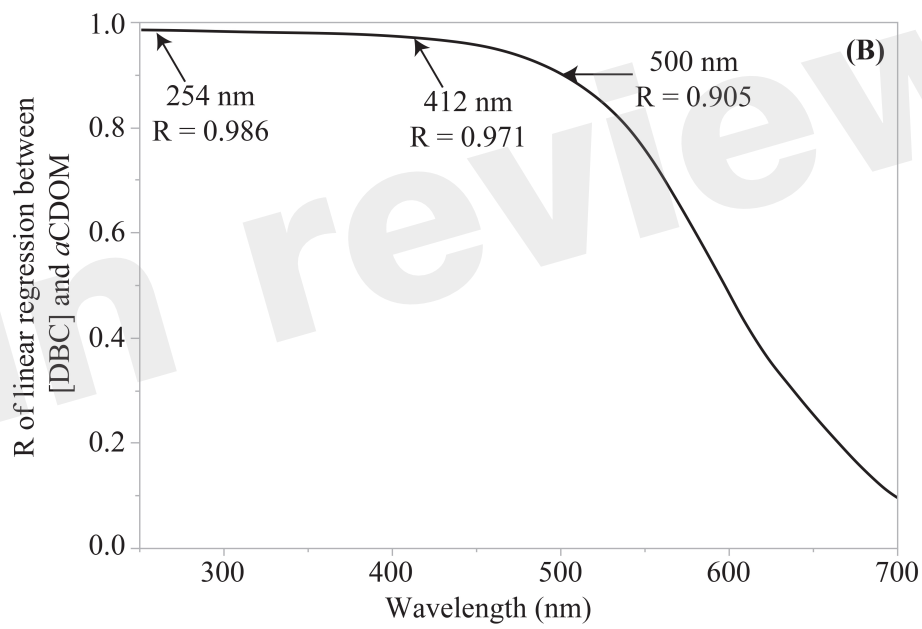
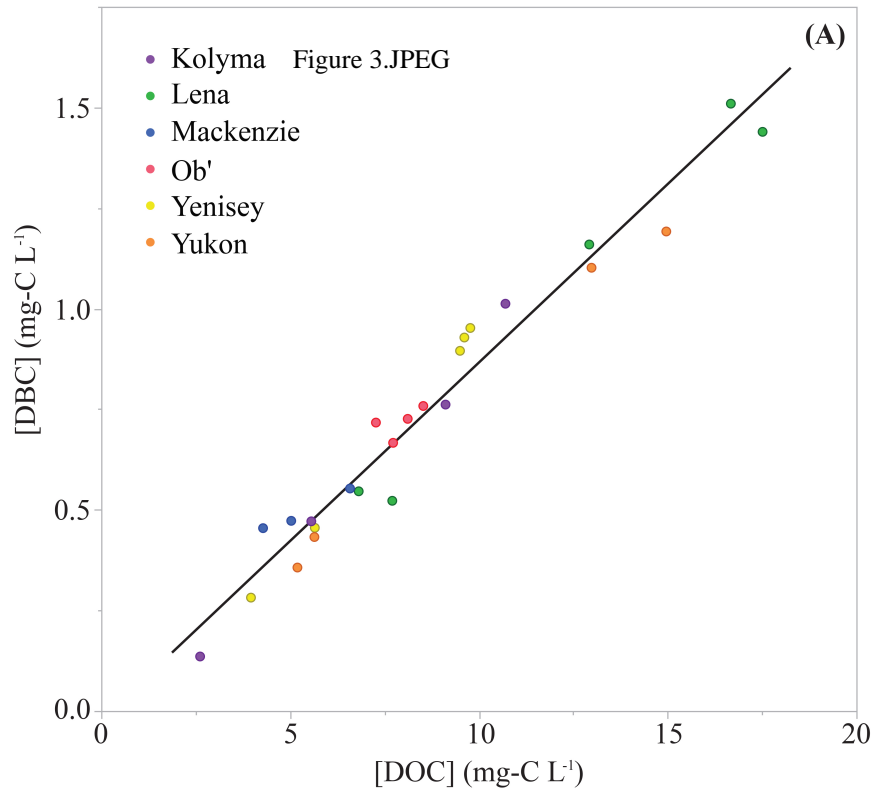


Figure 4.JPEG

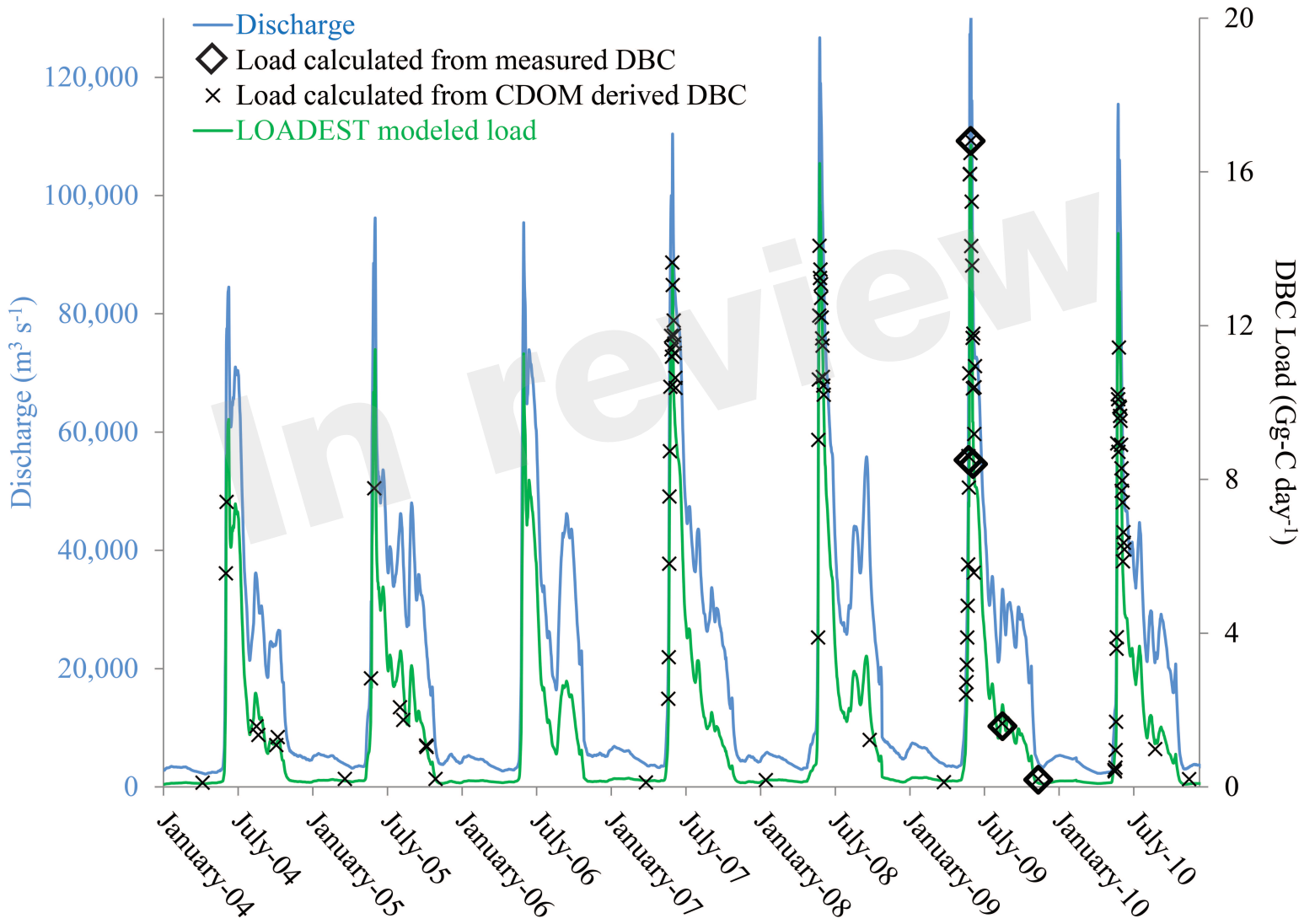




Figure 5.JPEG

